

RESEARCH ARTICLE



## LncRNA SCARNA8 promotes atherosclerotic plaque instability by inhibiting macrophage efferocytosis

Xiaoliang Yin<sup>a\*</sup>, Xiaodong Chen<sup>a\*</sup>, Tao Wang<sup>a</sup>, Jianling Yang<sup>a</sup>, Jiahui Yu<sup>a</sup>, and Jun Yang<sup>a,b</sup>

<sup>a</sup>Department of Neurosurgery, Peking University Third Hospital, Beijing, China; <sup>b</sup>Center for Precision Neurosurgery and Oncology, Peking University Health Science Center, Beijing, China

### ABSTRACT

In recent years, findings suggest that long noncoding RNAs (lncRNAs) are closely related to the development of atherosclerosis (AS), but there is a lack of studies on the involvement of lncRNA-regulated cytosolic burial in the regulation of AS. In this study, we investigated the mechanism by which lncRNA SCARNA8 affects macrophage cell burial to regulate AS. The cytosolic burial-associated target gene regulated by lncRNA SCARNA8 was PPARG. lncRNA SCARNA8 was increased in the carotid unstable plaque group, whereas PPARG was decreased. Ox-LDL led to the up-regulation of lncRNA SCARNA8 expression and apoptosis in Raw264.7 cells in a time-, concentration-dependent manner. Knockdown of lncRNA SCARNA8 upregulated PPARG and reduced apoptosis in Raw264.7 cells. In addition, knockdown of lncRNA SCARNA8 improved the stability of atherosclerotic plaques by promoting cellular burial of Raw264.7 cells. lncRNA SCARNA8 is a key regulator of plaque vulnerability, and targeting lncRNA SCARNA8 May provide a novel means for the prevention and treatment of AS.

### ARTICLE HISTORY

Received 20 September 2024  
Revised 3 March 2025  
Accepted 26 March 2025

### KEYWORDS



Long noncoding RNAs; atherosclerosis; macrophage efferocytosis; PPARG

## Introduction


Atherosclerosis (AS) is a slow-progressing, chronic inflammatory disease characterized by endothelial dysfunction, lipid infiltration, and foam cell production, leading to the formation of atherosclerotic plaques, which in turn leads to hardening, stenosis, and thrombosis of the vascular wall [1,2]. Atherosclerotic plaque instability is the main cause of AS [3,4]. Although most atherosclerotic plaques remain relatively stable clinically, some unstable plaques may suddenly rupture after decades of slow progression, leading to life-threatening acute ischemic events [5,6]. The pathologic process includes multiple components such as vascular endothelial cell injury, inflammatory cell recruitment, increased macrophage death and impaired clearance, and its development is always accompanied by an inflammatory response, in which the interaction of macrophages, inflammatory factors, and inflammatory pathways that progressively amplify the inflammatory response is one of the most important factors leading

to progression of the plaque to instability and plaque rupture [7]. Studies have shown that the stability of plaques is mainly closely related to the morphological characteristics and major components of the plaque, including the size of the lipid core, the thickness of the fibrous cap, the degree of inflammatory cell aggregation, the content of matrix collagen, and the number of neovascularization within the plaque [8]. Therefore, early identification and stabilization of vulnerable plaques have important clinical significance and social value for patients at high risk of plaque rupture.

Long non-coding RNAs (lncRNAs) are a class of RNAs longer than 200 nucleotides that are currently thought to have no or minimal protein-coding capacity and are involved in epigenetic regulation by modulating gene expression [9]. There is increasing evidence that some AS-associated lncRNAs are involved in lipid homeostasis, such as cholesterol uptake, modified lipoprotein uptake, and reverse cholesterol transport, and thus influence the

**CONTACT** Jun Yang  [bysysjwk@126.com](mailto:bysysjwk@126.com)  Department of Neurosurgery, Peking University Third Hospital, No. 49 Huayuan North Road, Haidian District, Beijing 100191, China

\*These authors contributed equally.

 Supplemental data for this article can be accessed online at <https://doi.org/10.1080/15592294.2025.2487317>

© 2025 The Author(s). Published by Informa UK Limited, trading as Taylor & Francis Group.

This is an Open Access article distributed under the terms of the Creative Commons Attribution-NonCommercial License (<http://creativecommons.org/licenses/by-nc/4.0/>), which permits unrestricted non-commercial use, distribution, and reproduction in any medium, provided the original work is properly cited. The terms on which this article has been published allow the posting of the Accepted Manuscript in a repository by the author(s) or with their consent.

progression of AS [10,11]. In addition, recent studies have shown that lncRNAs are present in the circulation and can be used as independent biomarkers reflecting the local progression of cardiovascular disease [12,13]. Screening of lncRNAs in atherosclerotic ischemic stroke by gene microarray detection of whole blood RNA from subjects revealed that the lncRNA SCARNA8 was most significantly upregulated, suggesting that it may play an important role in the pathological process of atherosclerotic ischemic stroke [14].

In AS, uptake of oxidized lipoproteins by macrophages exceeds cholesterol efflux, leading to cholesterol ester deposition and subsequent foam cell formation [15,16]. Apoptosis secondary to foam cell necrosis is thought to be the primary cause of lipid core progression and vulnerable plaque formation [17,18]. Under physiological conditions, these apoptotic cells are rapidly removed by macrophages and other phagocytes in a process known as efferocytosis. Recent evidence has shown that in advanced plaques in humans and animals, defective cytosolic burial leads to a continuous accumulation of necrotic cells within the plaque, exacerbating the inflammatory response and plaque destabilization [19–21]. PPAR $\gamma$ , a regulator of lipid and glucose metabolism, has been found to be associated with AS and cytosolic burial [22]. Foam cell formation can be inhibited by activating the PPAR $\gamma$ -LXR $\alpha$ -ABCA1/G1 pathway. It also improves lipid metabolism and the inflammatory microenvironment, thus synergizing its anti-atherosclerotic effects [23]. Bioinformatics analysis revealed that the cytosolic burial-associated target gene regulated by SCARNA8 lncRNA is PPAR $\gamma$ . However, whether there is a targeted regulatory relationship between lncRNA SCARNA8 and PPAR $\gamma$ , and the specific mechanisms of both in macrophage cytosolic burial and atherosclerotic plaque instability are not clear. To address these questions, we preliminarily explored the mechanism of action of lncRNA SCARNA8 in clinical and in vitro atherosclerotic plaques.

## Materials and methods

### Data collection and processing

The dataset GSE43292 was obtained from the Gene Expression Omnibus (GEO) database ([https://](https://www.ncbi.nlm.nih.gov/gds)

[www.ncbi.nlm.nih.gov/gds](https://www.ncbi.nlm.nih.gov/gds)), which is a dataset of expression profiles of atherosclerotic plaque samples and intact tissue samples.

### Differential analysis of lncRNA

The GSE43292 expression profiling dataset was subjected to differential analysis using the R package ‘limma,’ the threshold of differentially expressed genes (DEGs) was set to  $|\log FC| > 0.585$  and  $p.adjust < 0.05$ . SCARNA8 differential expression boxplots were plotted using the R packages ggpubr and ggplot2.

### lncRNA target gene set

The target target genes were screened using the lncRNA2Target v3.0 database (<http://bio-annotation.cn/lncrna2target>) [24].

### Enrichment analysis

The Gene Ontology (GO) and Kyoto Encyclopedia of Genes and Genomes (KEGG) enrichment analysis of DEGs using the R package clusterProfiler, org.Hs.eg.db, and visualization using the R package enrichplot.

### Differential genes, intersection of cytosolic genes and target genes of SCARNA8

Cytosolic genes were obtained from the NCBI database (<https://www.ncbi.nlm.nih.gov/>), and cytosolic genes were obtained by screening the species ‘Homo sapiens,’ they were analyzed by using the website venn 2.0, Venny 2.1.0 (liuxiaoyuyuan.cn) for analysis.

### Patient sample preparation

The study included 21 patients with with unstable plaques of AS aged 65 years and 9 patients with stable plaques of AS aged 62 years. The male-to-female ratio was 9:1. All patients were from the department of Neurosurgery, Peking University Third Hospital. The patients with AS were confirmed by intracranial angiography and imaging. The patients included in this study constituted consecutive cases of carotid endarterectomy

(CEA). All patients had stenosis confirmed by bilateral carotid ultrasound, head and neck CTA, head MRA, or digital subtraction angiography (DSA) prior to surgery. The inclusion criteria for CEA surgery were as follows: I. The carotid artery stenosis rate was greater than 50% in symptomatic patients. In the case of asymptomatic patients, the carotid artery stenosis rate must be greater than 70%. The patient's general condition must allow them to undergo general anaesthesia and must have a life expectancy of more than five years. Exclusion criteria include: complete occlusion of the carotid artery; serious systemic diseases, such as severe coronary heart disease, heart failure (left ventricular ejection fraction less than 30%), severe chronic lung disease, uncontrolled diabetes or other systemic metabolic diseases. Furthermore, non-atherosclerotic stenosis, including conditions such as Takayasu arteritis and a history of cervical radiation therapy, was excluded from the study. We obtained demographic data and clinical information by analyzing the patients' medical record, and completed the patients' investigation of the medical history (Supplementary Table S1). Peripheral venous blood was collected from subjects for RNA extraction and subsequent analysis. The study was approved by Peking University Third Hospital. In addition, all signed informed consents were obtained from the study subjects.

**Sample collection and morphology** Carotid atherosclerotic plaque tissue samples were obtained from symptomatic patients who constituted consecutive cases of CEA. These samples were sourced from the Maastricht Pathology Tissue Collection (MPTC). The carotid plaque specimens were sectioned into parallel transverse segments, each measuring 5 mm in thickness. Subsequently, every other segment was rapidly frozen in liquid nitrogen and stored at  $-80^{\circ}\text{C}$ , while the adjacent segments were fixed in formalin for 24 h and then subjected to

decalcification for 4 h before being processed and embedded in paraffin for histological analysis.

### Cell culture

RAW 264.7 cells (Punosai Life Sciences, China) were grown in Dulbecco's minimum essential medium (DMEM) (Gibco) with 10% fetal bovine serum (FBS) (Excell Bio, China) and 1% penicillin-streptomycin (Beyotime, China) and cultured at  $37^{\circ}\text{C}$ , 5%  $\text{CO}_2$  in an incubator. When the cell density reached over 80%, the cells were dissociated using 1 mL of 0.25% trypsin (Gibco) for 60 seconds. Once the cells detached and became rounded, 5 mL of DMEM was added. Following this, the cells were transferred to culture flasks or 6-well plates for further cultivation. After the RAW 264.7 cells grew to 50–60% fusion, the inducer Oxidized Low-density Lipoprotein (ox-LDL) (0, 25, 50, 100, 150  $\mu\text{g/mL}$ , L34357, Thermofisher, USA) was added to establish an *in vitro* AS model.

For the co-culture of Raw 264.7 cells with bone marrow macrophages (BMDMs) (IMMOCELL, China), BMDMs ( $6 \times 10^3$  cells/well) were inoculated in 24-well plates overnight, and serum-free medium was changed 2 h before co-culture.

### Plasmid si-SCARNA8 knockdown construction

The construction of plasmid si-SCARNA8 (Suzhou Jimar Gene) was to insert si-SCARNA8 into pLKO.1 with siRNA construct. After construction, it was packaged into lentivirus using lentiviral packaging system. After obtaining the constructed lentiviral expression vector, it can be transfected into cells. The si-SCARNA8 and its negative control (NC) sequence is provided in the Table 1.

**Table 1.** Si-SCARNA8 sequence.

Plasmid	Sequence (5'-3')
si-SCARNA8	Forward: AAAGTGAGTTAAGCGGGACCATTCAAGAGATGGTCCCGCTTAACCTACTTT Reverse: GTCCCGCTTAACCTACTTTAGAAGTTCTCTCTAAAGTGAGTTAAGCGGGAC
si-NC	Forward: CACCGTTCTCCGAACGTGTACGTTTCAAGAGAACGTGACACGTTCCGAGAATTTTT G Reverse: GATCCAAAAAATCTCCGAACGTGTACGTTCTCTTGAACGTGACACGTTCCGAGAAC

### Cell transfection

When RAW 264.7 cells population reached to 70–80% confluence, si-SCARNA8 plasmid was used to infect RAW 264.7 cells and polybrene was added to enhance the viral transfection effect. The virus solution was withdrawn after 8 h, and the culture was switched to DMEM and continued for 24 h. Subsequently, the RAW 264.7 cells were switched to PURO-containing DMEM and continued to be cultured. After 7d, SCARNA8 knock-down RAW 264.7 cells were constructed.

### Real-time reverse transcription quantitative polymerase chain reaction (RT-qPCR)

The tissue samples and RAW 264.7 cells were employed to extract total RNA with Trizol reagent (10296028; Invitrogen). RNA purity was assessed by the absorbance ratio at 260 and 280 nm. Detection through RT-qPCR was done with the Platinum SYBR Green qPCR SuperMix-UDG kit (Invitrogen, USA). Gene expression levels were quantified using the  $2^{-\Delta\Delta C_t}$  method alongside internal controls like Glyceraldehyde-3-phosphate dehydrogenase (GAPDH) or endogenous small nuclear RNA U6. The primer sequence is provided in Table 2.

### Western blotting (WB)

Proteins were isolated by utilizing a cell lysis solution (Biosharp, China). The concentration of proteins was determined using the Bradford assay kit. After mixing thoroughly by vortex, equal amounts of proteins from each sample were analyzed by sodium dodecyl sulfate-

polyacrylamide gel electrophoresis (SDS-PAGE) and transferred to polyvinylidene fluoride (PVDF) membranes (NCM Biotech, China). The PVDF membranes were then blocked with 5% skim milk and incubated overnight at 4°C with antibodies targeting PPARG, TNF- $\alpha$ , GAS6 (1:1000, Thermofisher, USA; Abcam, UK; proteintech, China) and MFGE8 (1:1000, Abcam, UK). Subsequently, a 2-hour incubation was carried out with a secondary antibody at a 1:10000 dilution (Bioss, China). The signal was visualized using an enhanced chemiluminescence kit (NCM Biotech, China).

### MTT cell proliferation and cytotoxicity assay

RAW 264.7 cells ( $6 \times 10^3$  cells/well) were seeded in 96-well plates. After cell attachment, MTT cell proliferation and cytotoxicity assay kit (Beyotime, China) was added to RAW 264.7 cells. The amount of MTT solution added to each well is 10  $\mu$ l at a concentration of 0.5 mg/ml. The MTT reaction time is 4 h, MTT will be taken up by the cells and reduced to purple methyl formate. Methyl formate was solubilized by adding 100  $\mu$ l of DMSO dissolution solution and the IC<sub>50</sub> of the cells was determined by measuring the OD value.

### Flow cytometry (FCM)

RAW 264.7 cells were extracted and centrifuge for 5 minutes. Remove the supernatant, rinse the cells with 1 mL of PBS and centrifuge again. Cell suspensions were prepared according to Annexin V, FITC/PI Apoptosis Detection Kit (DOJINDO, Japan). RAW 264.7 cells were labeled with pHrodo Green (Thermo Fisher Scientific, USA) and unphagocytosed apoptotic RAW 264.7 cells were removed by PBS after co-culture and incubation with BMDMs for 2 h, respectively. Apoptosis and cellular burial were detected on an Attune NxT flow cytometer.

### Immunofluorescence (IF)

RAW 264.7 cells were labeled using 2.5  $\mu$ M live cell fluorescent dye CFSE (Life Technologies, Burlington, Ontario, Canada). After co-culture with

**Table 2.** Primer sequence.

Primer	Sequence (5'-3')
SCARNA8	Forward: G T A C T G C T C C A G T T G T C A C T Reverse: A T T G T C T G C C C C G T A T C T G T C
TNF- $\alpha$	Forward: C C C T C A C T C A C A A C C A C Reverse: A C A A G G T A C A C C C A T C G G C
FG-E8	Forward: C A C A G C C G T C C C C A A T A C T Reverse: G A C G A G G C G G A A A T C T G T G A
GAS6	Forward: A T G A A G A T C G C G G T A G C T G G Reverse: G C C A A C T C C T C A T G C A C C C A T
PPARG	Forward: C T G T G A G A C C A A C A G C C T G A Reverse: A A G T T G G T G G G C C A G A A T G G
GAPDH	Forward: C C C T T A A G A G G G A T G C T G C C Reverse: T A C G G C C A A T C C G T T C A C A



BMDMs, unphagocytosed apoptotic RAW 264.7 cells were removed by PBS. Inverted fluorescence microscopy was performed and imaged. The phagocytosis index is defined as the number of apoptotic cells containing CFSE+ per 100 BMDMs.

### Statistical analysis

Data were analyzed and plotted using GraphPad Prism 9 (Version 9.4.0), and figures were organized using Adobe Illustrator 2023. Mean values with standard deviations (SD) were used to display the data. T-tests were employed for comparing two groups, and ANOVA tests were utilized for comparisons across multiple groups. Statistical significance was determined at a threshold of  $p < 0.05$ .

## Result

### Identification of SCARNA8 target genes associated with cellular burials

The dataset of GSE43292 was obtained from the GEO database, which contained 64 samples, including 32 atherosclerotic tissue samples (AS) and 32 control samples (NAS), and a total of 25,279 genes were obtained after screening, and the expression profiles of the screened samples were normalized using the R package 'limma' (Figure 1(a)). The R package 'limma' was used to identify 950 DEGs between NAS and AS groups, which were visualized by volcano plots, including 558 differentially up-regulated genes and 392 differentially down-regulated genes (Figure 1(b)). The grouped box line plots showed that SCARNA8 was significantly different between the AS and NAS groups (Figure 1(c)). The results of GO enrichment analysis indicated that DEGs were significantly enriched in the immune response-regulating signaling pathway (Figure 1(d)). The results of KEGG enrichment analysis showed that DEGs were mainly enriched in the Cytokine-cytokine receptor interaction (Figure 1(e)). The target genes of SCARNA8 were screened according to the results of LncRNA2Target V3.0 database assay, and finally 2572 differentially expressed target genes were collected from the database. Subsequently, the intersection gene PPARG between differentially expressed target genes, cytosolic burial cytosolic burial genes, and DEGs was

screened by plotting the Wayne diagram, and it was used as a SCARNA8-related cytosolic burial-related gene (Figure 1(f)).

### Patients with unstable atherosclerotic plaques had elevated levels of lncRNA SCARNA8 in peripheral blood and tissue does

The presence of unstable plaques was confirmed according to color ultrasound and MRI in the unstable plaque group ( $n = 21$ ), while the stable plaque negative control group ( $n = 9$ ) was confirmed to have stable plaques. Peripheral blood and carotid plaque tissues were collected from patients, and RT-qPCR analysis demonstrated that the levels of lncRNA SCARNA8 in the peripheral blood and tissues of patients in the unstable plaque group were significantly higher than those in the stable plaque group, whereas PPARG was downregulated (Figure 2a,b). The protein expression of PPARG in the unstable plaque group was found to be consistent with the mRNA expression, as determined by WB testing of patients' carotid plaque tissues (Figure 2c). This suggests that lncRNA SCARNA8 May be associated with atherosclerotic stability in clinical practice.

### Apoptosis and the expression pattern of lncRNA SCARNA8 in an in vitro as model

Previous studies have shown that ox-LDL plays an important role in the formation of atherosclerotic lesions. Therefore, to mimic apoptotic macrophages within atherosclerotic plaques in vitro, RAW 264.7 cells were stimulated with different concentrations of ox-LDL and different intervention times. The MTT assay revealed that cell viability was reduced (Figure 3(a,b)). The RT-qPCR assay demonstrated that ox-LDL could lead to the up-regulation of the expression of lncRNA SCARNA8 in a time- and concentration-dependent manner (Figure 3(c,d)). Furthermore, the results indicated that the optimal induction concentration and time of ox-LDL was 100  $\mu\text{g/mL}$  for 24 h. Apoptosis was observed to occur following ox-LDL induction, as determined by FCM (Figure 3(e)).

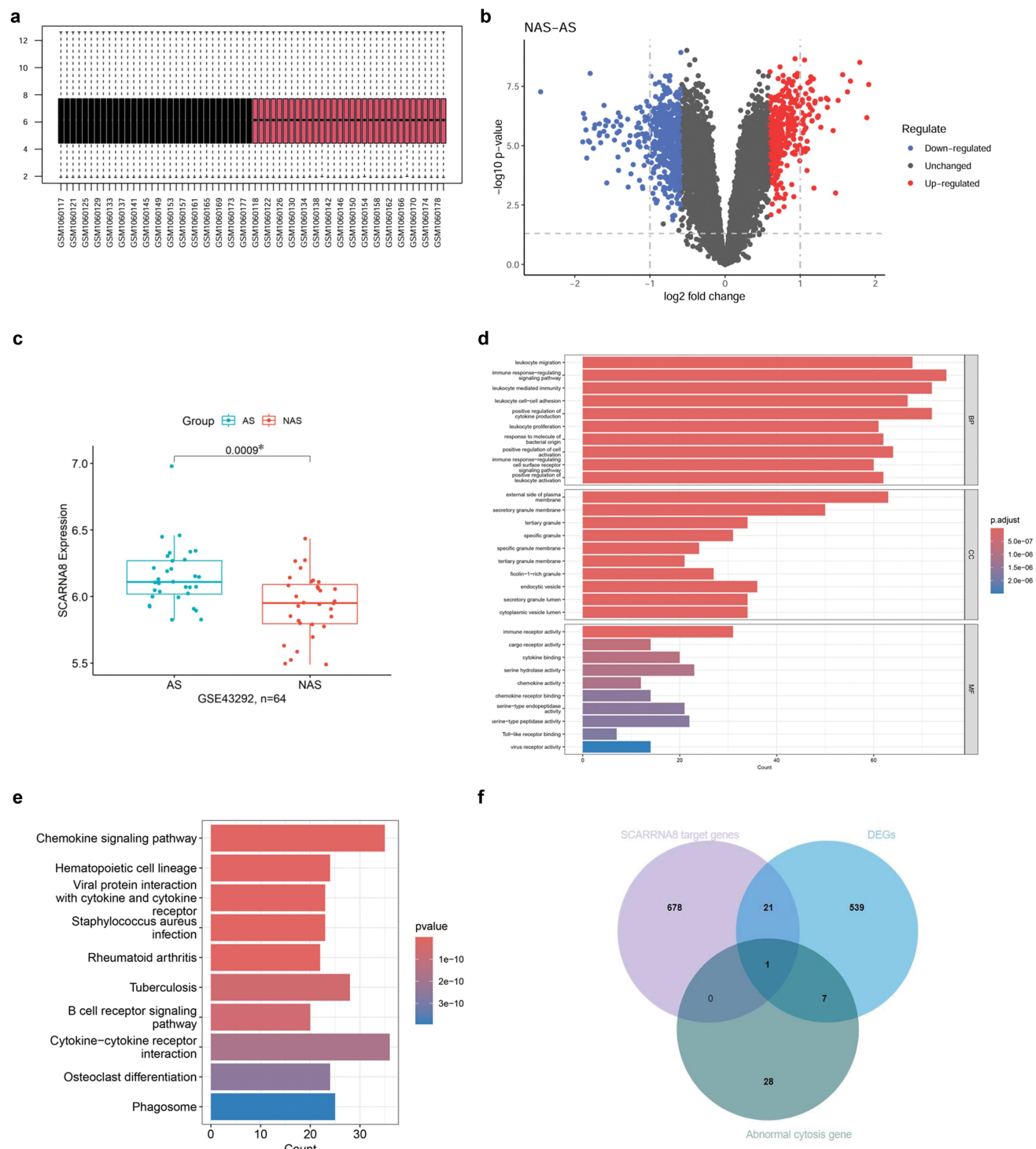


**Figure 1.** Identification of SCARNA8 target genes associated with cellular burials. (a) Normalized data boxplot (black: NAS group, red: AS group). (b) Volcano plot of GSE43292 intergroup difference analysis (blue dots: down-regulated genes, gray dots: unchanged genes, red dots: up-regulated genes). (c) Box line plot of LncRNA SCARNA8 expression in the two groups. (d) Histogram of GO enrichment analysis results. (e) Histogram of KEGG enrichment analysis results. (f) Wayne plots of differentially expressed target genes, cytosolic burial genes, DEGs.

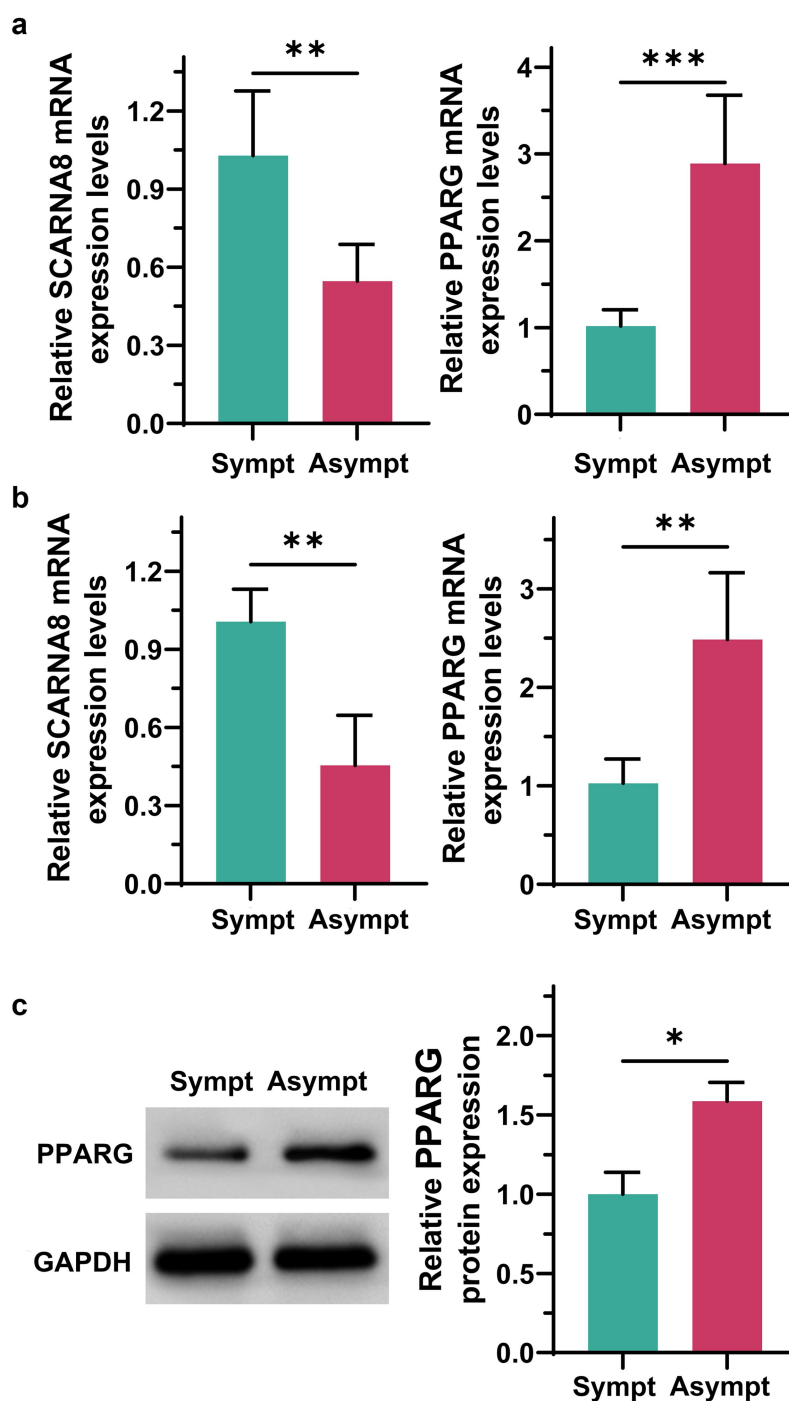


**Figure 2.** Patients with unstable atherosclerotic plaques had elevated levels of lncRNA SCARNA8 in peripheral blood and tissue does. (a) lncRNA mRNA SCARNA8 and PPARG cRNA levels of peripheral blood of patients with unstable atherosclerotic plaques. (b) lncRNA mRNA SCARNA8 and PPARG mRNA levels of tissue does of patients with unstable atherosclerotic plaques. (c) PPARG protein level of tissue does of patients with unstable atherosclerotic plaques. Data are reported as means  $\pm$  SD with three replicates. \* $p < 0.05$ , \*\* $p < 0.01$ , \*\*\* $p < 0.001$ .

### Knockdown of lncRNA SCARNA8 attenuates apoptosis in vitro

RT-qPCR confirmed the effectiveness of si-SCARNA8 (Figure 4(a)). To investigate whether

si-SCARNA8 could ameliorate apoptosis in RAW 264.7 cells, cell viability was detected by MMT and FCM, as well as apoptosis-related genes were detected by RT-qPCR and WB, and it was found

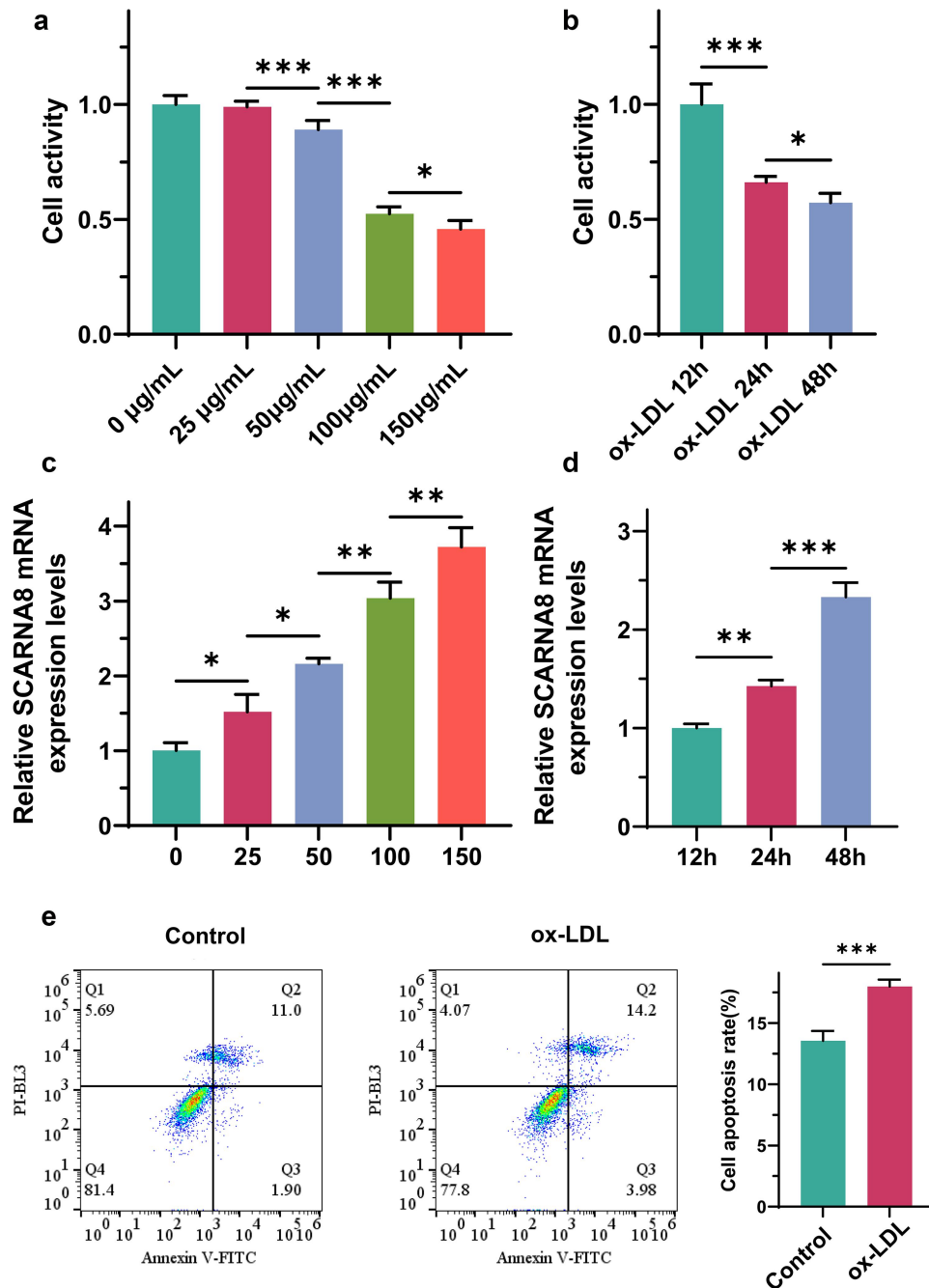


**Figure 3.** Apoptosis and the expression pattern of lncRNA SCARNA8 in an in vitro as model. (a) Cell activity of different concentrations of ox-Ldl on Raw264.7 cells. (b) Cell activity of ox-Ldl on Raw264.7 cells at different induction times. (c) lncRNA SCARNA8 mRNA levels of different concentrations of ox-Ldl on Raw264.7 cells. (d) lncRNAmRNA SCARNA8 mL levels of ox-Ldl on Raw264.7 cell at different induction times. (e) FCM of 100 μg/undefined ox-Ldl on Raw264.7 cells. Data are reported as means  $\pm$  SD with three replicates. \* $p < 0.05$ , \*\* $p < 0.01$ , \*\*\* $p < 0.001$ .

that knocking down the lncRNA SCARNA8 after ox-LDL induction promoted cell proliferation and reduced apoptosis, compared with the induction group (Figure 4(b,c)). In addition, knockdown of lncRNA SCARNA8 down-regulated the expression of TNF- $\alpha$  and up-regulated the expression of

MFG-E8, GAS6, and PPARG at the mRNA level and protein level (Figure 4(d,h)). This suggests that knockdown of lncRNA SCARNA8 attenuated RAW 264.7 apoptosis in an in vitro AS model, in which lncRNA SCARNA8 and PPARG may have a targeting relationship.



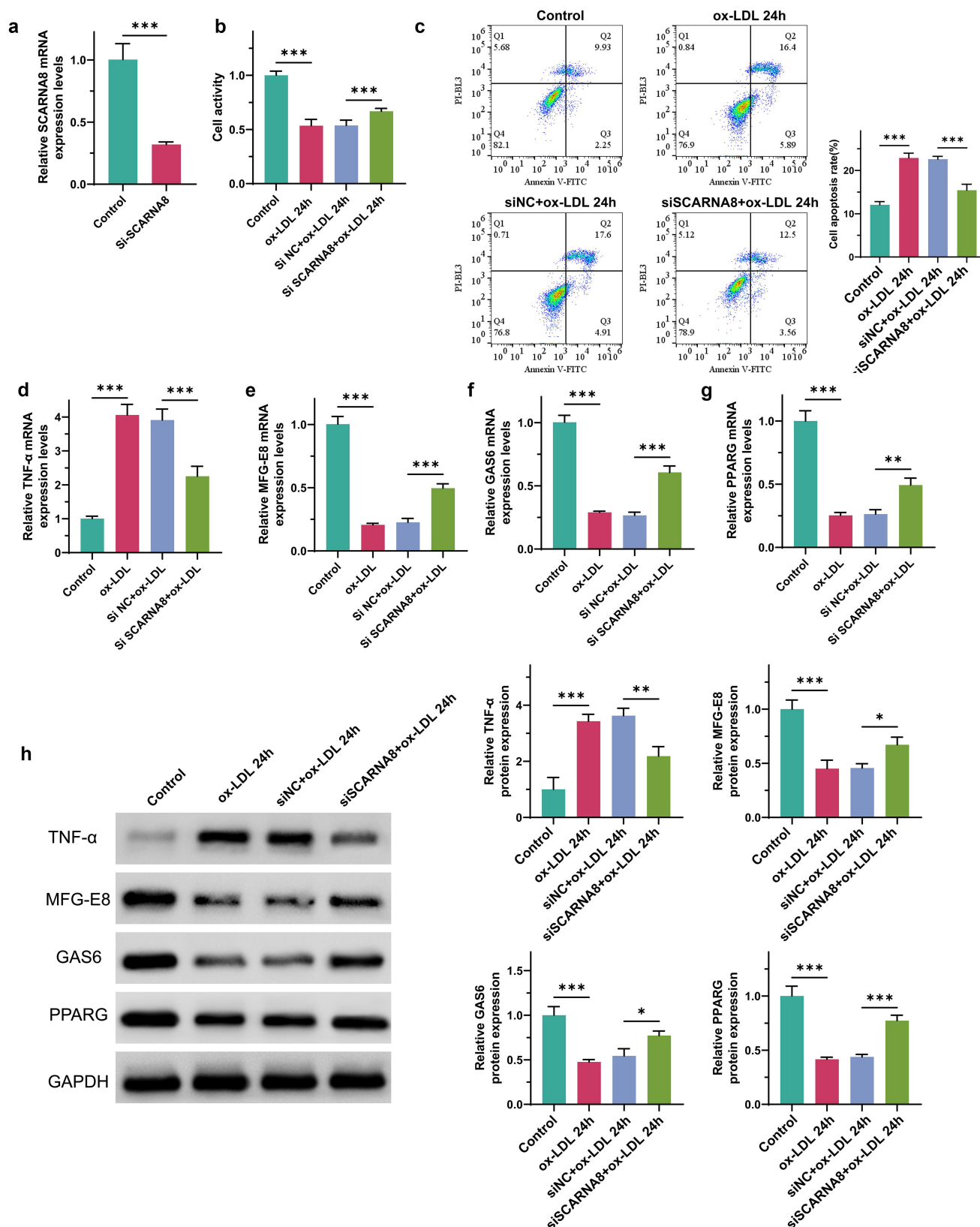


**Figure 4.** Knockdown of lncRNA SCARNA8 attenuates apoptosis in vitro. (a) lncRNA mRNA SCARNA8 cRNA levels after knockdown. (b) Cell activity of ox-LDL on Raw264.7 cells after lncRNA SCARNA8 knockdown. (c) FCM of ox-LDL on Raw264.7 cells after lncRNA SCARNA8 knockdown. (d-g) *tnf- $\alpha$* , *MFG-E8*, *GAS6* and *PPARG* cRNA levels of ox-LDL on Raw264.7 cells after lncRNA SCARNA8 knockdown. (h) *TNF- $\alpha$* , *MFG-E8*, *GAS6* and *PPARG* protein levels of ox-LDL on Raw264.7 cells after lncRNA SCARNA8 knockdown. Data are reported as means  $\pm$  SD with three replicates. \* $p < 0.05$ , \*\* $p < 0.01$ , \*\*\* $p < 0.001$ .

### ***Knockdown of lncRNA SCARNA8 promotes cell burial in apoptotic macrophage in vitro***

To investigate whether lncRNA SCARNA8 improved the stability of atherosclerotic plaques by promoting RAW 264.7 cell cyto-burial and thereby improving the stability of atherosclerotic plaques, IF and FCM assays were used and found that si-SCARNA8 effectively enhanced the cyto-burial of apoptotic macrophages (Figure 5(a,b)).

### **Discussion**

In this study, bioinformatics analysis revealed that the cell-cell burial-associated target gene regulated by lncRNA SCARNA8 is PPARG. We verified the correlation between lncRNA SCARNA8 and the stability of atherosclerotic plaques from clinical and in vitro experiments, respectively, and further demonstrated that it can promote macrophage cell-cell burial through knocking down lncRNA SCARNA8 in cell burial and thereby ameliorating atherosclerotic plaque instability, which may be achieved by targeting PPARG.

LlncRNAs play a role in a multitude of biological regulatory functions, particularly at the epigenetic, transcriptional, and post-transcriptional levels, as well as in other aspects of biological processes [25]. It has been demonstrated that lncRNA plays a pivotal role in the pathogenesis of cardiovascular diseases, particularly in the context of coronary atherosclerotic heart disease [26]. The presence of circulating blood lncRNA can be utilized for the early diagnosis of disease, suggesting disease development. Li et al. demonstrated that the expression of lncRNA NEAT1 in the peripheral blood of patients with ischemic stroke was higher than that of normal control patients, and that lncRNA NEAT1 was positively correlated with inflammatory factors such as CRP, TNF- $\alpha$ , IL-6, IL-8, IL-22, etc. Furthermore, a negative correlation was observed between lncRNA NEAT1 and the inflammatory inhibitory factor IL-10, indicating that lncRNA NEAT1 May serve as a novel biomarker for predicting the risk of ischemic stroke and monitoring disease severity, inflammation levels, and prognosis in this condition [27]. Furthermore, apoptosis, oxidative stress, and adhesion molecule release in HUVEC were

alleviated by lncRNA MIR4697HG in an in vitro model. In an in vivo model, it was observed that lncRNA MIR4697HG could alleviate the progression of atherosclerosis in mice through the FUS/ANXA5 axis [28]. In this study, we analyzed the expression of lncRNA SCARNA8 in peripheral blood and plaque tissues of patients with acute ischemic stroke and further validated it in an in vitro AS model. Our findings suggest that lncRNA SCARNA8 is an important lncRNA that correlates with the stability of atherosclerosis, and that its expression is increased and released into the pericellular environment. lncRNA SCARNA8 May serve as a novel indicator for the early diagnosis of acute ischemic stroke and the evaluation of arterial plaque stability.

Previous studies have demonstrated that the components of atherosclerotic plaques, such as the necrotic core composed of apoptotic cells, are the primary contributors to their destabilization [29]. In contrast, atherosclerosis is a lipid-driven inflammatory disease of the arterial intima, where the balance of pro- and anti-inflammatory mechanisms determines the final clinical outcome [30]. Endothelial infiltration and modification of plasma-derived lipoproteins and their uptake mainly by macrophages, followed by the formation of lipid-filled foam cells, initiate the formation of atherosclerotic lesions. Insufficient in vitro cellular clearance of apoptotic and foam cells can promote plaque progression. Defective cytosolic burial, a hallmark of inadequate inflammatory abatement, can lead to secondary accumulation of necrotic macrophages and foam cells and formation of advanced lesions with a necrotic lipid core, suggesting plaque vulnerability [7]. In this study, we constructed an in vitro AS model using ox-LDL-treated macrophages, which resulted in upregulation of Raw264.7 cell lncRNA SCARNA8 expression in a time- and concentration-dependent manner. The results of the MTT, FCM, RT-qPCR, and WB assays indicated that the knockdown of lncRNA SCARNA8 reduced macrophage apoptosis and increased macrophage clearance of apoptotic cells. These findings suggest that the knockdown of lncRNA SCARNA8 could slow down the progression of atherosclerosis and increase plaque stability. Additionally, this may explain the observed decrease in necrotic core and the increase in plaque stability.

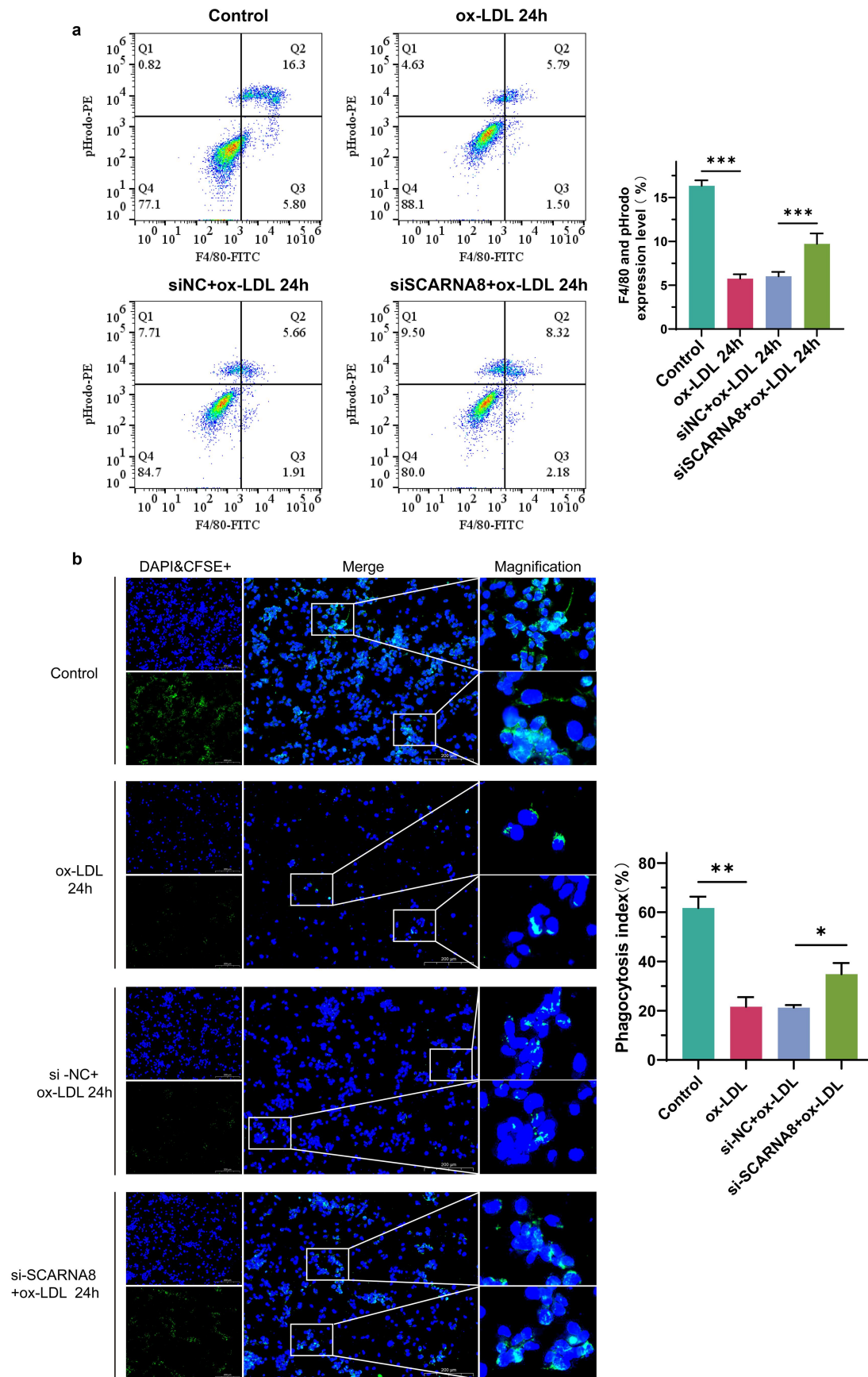


**Figure 5.** Knockdown of lncRNA SCARNA8 promotes cell burial in apoptotic macrophage in vitro. (a) FCM of cellular burial of ox-Ldl on Raw264.7 cells after lncRNA SCARNA8 knockdown. (b) immunofluorescence diagram of TUNEL staining, green fluorescence represents TUNEL, and blue fluorescence represents DAPI. Scale bar is 200  $\mu$ m. Statistics of cell apoptosis based on TUNEL immunofluorescence. Data are reported as means  $\pm$  SD with three replicates. \* $p < 0.05$ , \*\* $p < 0.01$ , \*\*\* $p < 0.001$ .

One of the primary causes of the enlargement of the necrotic core is the malfunctioning of the cellular components in advanced atherosclerotic plaques. This results in an increasing accumulation of apoptotic cells within the plaque, impaired clearance, and an inflammatory second necrotic core caused by apoptosis. Ultimately, this leads to the destabilization of the plaque [31]. To elucidate the mechanism through which si-SCARNA8 enhances the stability of atherosclerotic plaques, we observed that si-SCARNA8 stimulates macrophage proliferation via flow cytometry and immunofluorescence analysis. pPARG exhibited a correlation with cellular proliferation. Dolichosperm methylin exerts a protective effect against atherosclerosis by regulating the formation of foam macrophages and the inflammatory response through the FABP4/PPARG signaling pathway [32]. In allergic asthma, PGRN deficiency enhances cytosolic burial via the PPARG/MFG-E8 pathway, which may contribute to the suppression of respiratory inflammation in allergic asthma due to PGRN deficiency [33]. The ability of macrophages to undergo cell death in a lupus mouse model can be restored by activating the PPARG/LxR signaling pathway [34]. In this study, we confirmed the targeting relationship between lncRNA SCARNA8 and PPARG by bioinformatics, and also found that knockdown of lncRNA SCARNA8 upregulated the expression of PPARG, which was decreased in atherosclerotic plaque instability, by RT-qPCR and WB assay. lncRNA SCARNA8 may promote macrophage cell death and thus provide atherosclerotic plaque stability by targeting PPARG, but the specific molecular mechanisms need to be further explored.

## Disclosure statement

No potential conflict of interest was reported by the author(s).

## Funding

The work was supported by the National Natural Science Foundation of China [82071308].

## Data availability statement

The data that support the findings of this study are available on request from the corresponding author, [Jun Yang], upon reasonable request.

## References

- [1] Libby P, Buring JE, Badimon L, et al. Atherosclerosis. *Nat Rev Dis Primers*. 2019;5(1):56. doi: [10.1038/s41572-019-0106-z](https://doi.org/10.1038/s41572-019-0106-z)
- [2] Zhao L, Ma D, Wang L, et al. Metabolic changes with the occurrence of atherosclerotic plaques and the effects of statins. *Front Immunol*. 2023;14:1301051. doi: [10.3389/fimmu.2023.1301051](https://doi.org/10.3389/fimmu.2023.1301051)
- [3] Fowkes FG, Rudan D, Rudan I, et al. Comparison of global estimates of prevalence and risk factors for peripheral artery disease in 2000 and 2010: a systematic review and analysis. *Lancet*. 2013;382(9901):1329–1340. doi: [10.1016/S0140-6736\(13\)61249-0](https://doi.org/10.1016/S0140-6736(13)61249-0)
- [4] Ridker PM, Everett BM, Thuren T, et al. Antiinflammatory therapy with canakinumab for atherosclerotic disease. *N Engl J Med*. 2017;377(12):1119–1131. doi: [10.1056/NEJMoa1707914](https://doi.org/10.1056/NEJMoa1707914)
- [5] Toutouzas K, Benetos G, Karanasos A, et al. Vulnerable plaque imaging: updates on new pathobiological mechanisms. *Eur Heart J*. 2015;36(45):3147–3154. doi: [10.1093/eurheartj/ehv508](https://doi.org/10.1093/eurheartj/ehv508)
- [6] Lerman JB, Joshi AA, Chaturvedi A, et al. Coronary plaque characterization in psoriasis reveals high-risk features that improve after treatment in a prospective observational study. *Circulation*. 2017;136(3):263–276. doi: [10.1161/CIRCULATIONAHA.116.026859](https://doi.org/10.1161/CIRCULATIONAHA.116.026859)
- [7] Back M, Yurdagul A Jr., Tabas I, et al. Inflammation and its resolution in atherosclerosis: mediators and therapeutic opportunities. *Nat Rev Cardiol*. 2019;16(7):389–406. doi: [10.1038/s41569-019-0169-2](https://doi.org/10.1038/s41569-019-0169-2)
- [8] Wang F, Zhang Z, Fang A, et al. Macrophage foam cell-targeting immunization attenuates atherosclerosis. *Front Immunol*. 2018;9:3127. doi: [10.3389/fimmu.2018.03127](https://doi.org/10.3389/fimmu.2018.03127)
- [9] Kopp F, Mendell JT. Functional classification and experimental dissection of long noncoding RNAs. *Cell*. 2018;172(3):393–407. doi: [10.1016/j.cell.2018.01.011](https://doi.org/10.1016/j.cell.2018.01.011)
- [10] Kumar S, Williams D, Sur S, et al. Role of flow-sensitive microRNAs and long noncoding RNAs in vascular dysfunction and atherosclerosis. *Vascul Pharmacol*. 2019;114:76–92. doi: [10.1016/j.vph.2018.10.001](https://doi.org/10.1016/j.vph.2018.10.001)
- [11] Sallam T, Sandhu J, Tontonoz P. Long noncoding RNA discovery in cardiovascular disease: decoding form to function. *Circ Res*. 2018;122(1):155–166. doi: [10.1161/CIRCRESAHA.117.311802](https://doi.org/10.1161/CIRCRESAHA.117.311802)
- [12] Bayoumi AS, Aonuma T, Teoh JP, et al. Circular noncoding RNAs as potential therapies and circulating biomarkers for cardiovascular diseases. *Acta Pharmacol Sin*. 2018;39(7):1100–1109. doi: [10.1038/aps.2017.196](https://doi.org/10.1038/aps.2017.196)
- [13] Lucas T, Bonauer A, Dimmeler S. RNA therapeutics in cardiovascular disease. *Circ Res*. 2018;123(2):205–220. doi: [10.1161/CIRCRESAHA.117.311311](https://doi.org/10.1161/CIRCRESAHA.117.311311)
- [14] Ruan W, Wu J, Su J, et al. Altered lncRNAs transcriptional profiles in atherosclerosis-induced ischemic stroke. *Cell Mol Neurobiol*. 2022;42(1):265–278. doi: [10.1007/s10571-020-00918-y](https://doi.org/10.1007/s10571-020-00918-y)



- [15] Koelwyn GJ, Corr EM, Erbay E, et al. Regulation of macrophage immunometabolism in atherosclerosis. *Nat Immunol.* **2018**;19(6):526–537. doi: [10.1038/s41590-018-0113-3](https://doi.org/10.1038/s41590-018-0113-3)
- [16] Tabas I, Lichtman AH. Monocyte-macrophages and T cells in atherosclerosis. *Immunity.* **2017**;47(4):621–634. doi: [10.1016/j.immuni.2017.09.008](https://doi.org/10.1016/j.immuni.2017.09.008)
- [17] Kasikara C, Doran AC, Cai B, et al. The role of non-resolving inflammation in atherosclerosis. *J Clin Invest.* **2018**;128(7):2713–2723. doi: [10.1172/JCI97950](https://doi.org/10.1172/JCI97950)
- [18] Silvestre-Roig C, de Winther MP, Weber C, et al. Atherosclerotic plaque destabilization: mechanisms, models, and therapeutic strategies. *Circ Res.* **2014**;114(1):214–226. doi: [10.1161/CIRCRESAHA.114.302355](https://doi.org/10.1161/CIRCRESAHA.114.302355)
- [19] Arslan S, Berkan O, Lalem T, et al. Long non-coding RNAs in the atherosclerotic plaque. *Atherosclerosis.* **2017**;266:176–181. doi: [10.1016/j.atherosclerosis.2017.10.012](https://doi.org/10.1016/j.atherosclerosis.2017.10.012)
- [20] Doran AC, Ozcan L, Cai B, et al. CAMKII $\gamma$  suppresses an efferocytosis pathway in macrophages and promotes atherosclerotic plaque necrosis. *J Clin Invest.* **2017**;127(11):4075–4089. doi: [10.1172/JCI94735](https://doi.org/10.1172/JCI94735)
- [21] Seneviratne AN, Edsfeldt A, Cole JE, et al. Interferon regulatory factor 5 controls necrotic core formation in atherosclerotic lesions by impairing efferocytosis. *Circulation.* **2017**;136(12):1140–1154. doi: [10.1161/CIRCULATIONAHA.117.027844](https://doi.org/10.1161/CIRCULATIONAHA.117.027844)
- [22] Janani C, Ranjitha Kumari BD. PPAR gamma gene—a review. *Diabetes Metab Syndr.* **2015**;9(1):46–50. doi: [10.1016/j.dsx.2014.09.015](https://doi.org/10.1016/j.dsx.2014.09.015)
- [23] Wang SQ, Xiang J, Zhang GQ, et al. Essential oil from *Fructus Alpinia zerumbet* ameliorates atherosclerosis by activating PPAR $\gamma$ -LXR $\alpha$ -ABCA1/G1 signaling pathway. *Phytomedicine.* **2024**;123:155227. doi: [10.1016/j.phymed.2023.155227](https://doi.org/10.1016/j.phymed.2023.155227)
- [24] Cheng L, Wang P, Tian R, et al. LncRNA2Target v2.0: a comprehensive database for target genes of lncRNAs in human and mouse. *Nucleic Acids Res.* **2019**;47(D1):D140–D144. doi: [10.1093/nar/gky1051](https://doi.org/10.1093/nar/gky1051)
- [25] Fok ET, Davignon L, Fanucchi S, et al. The lncRNA connection between cellular metabolism and epigenetics in trained immunity. *Front Immunol.* **2018**;9:3184. doi: [10.3389/fimmu.2018.03184](https://doi.org/10.3389/fimmu.2018.03184)
- [26] Zhang D, Wang B, Ma M, et al. lncRNA HOTAIR protects myocardial infarction rat by sponging miR-519d-3p. *J Cardiovasc Transl Res.* **2019**;12(3):171–183. doi: [10.1007/s12265-018-9839-4](https://doi.org/10.1007/s12265-018-9839-4)
- [27] Li P, Duan S, Fu A. Long noncoding RNA NEAT1 correlates with higher disease risk, worse disease condition, decreased miR-124 and miR-125a and predicts poor recurrence-free survival of acute ischemic stroke. *J Clin Lab Anal.* **2020**;34(2):e23056. doi: [10.1002/jcla.23056](https://doi.org/10.1002/jcla.23056)
- [28] Liu X, Huang R, Wan J, et al. lncRNA MIR4697HG alleviates endothelial cell injury and atherosclerosis progression in mice via the FUS/ANXA5 axis. *Biochem Genet.* **2023**. 62 4 3155–3173. doi: [10.1007/s10528-023-10542-2](https://doi.org/10.1007/s10528-023-10542-2)
- [29] Ambale-Venkatesh B, Liu CY, Liu YC, et al. Association of myocardial fibrosis and cardiovascular events: the multi-ethnic study of atherosclerosis. *Eur Heart J - Cardiovasc Imaging.* **2019**;20(2):168–176. doi: [10.1093/ehjci/jez140](https://doi.org/10.1093/ehjci/jez140)
- [30] Yu XH, Zhang DW, Zheng XL, et al. Cholesterol transport system: an integrated cholesterol transport model involved in atherosclerosis. *Prog Lipid Res.* **2019**;73:65–91. doi: [10.1016/j.plipres.2018.12.002](https://doi.org/10.1016/j.plipres.2018.12.002)
- [31] Kojima Y, Weissman IL, Leeper NJ. The role of efferocytosis in atherosclerosis. *Circulation.* **2017**;135(5):476–489. doi: [10.1161/CIRCULATIONAHA.116.025684](https://doi.org/10.1161/CIRCULATIONAHA.116.025684)
- [32] Zhang M, Hou L, Tang W, et al. Oridonin attenuates atherosclerosis by inhibiting foam macrophage formation and inflammation through FABP4/PPAR $\gamma$  signalling. *J Cell Mol Med.* **2023**;27(24):4155–4170. doi: [10.1111/jcmm.18000](https://doi.org/10.1111/jcmm.18000)
- [33] Huang Q, Weng D, Yao S, et al. Progranulin deficiency suppresses allergic asthma and enhances efferocytosis via PPAR- $\gamma$ /MFG-E8 regulation in macrophages. *Immun Inflamm Dis.* **2023**;11(2):e779. doi: [10.1002/iid3.779](https://doi.org/10.1002/iid3.779)
- [34] Harder JW, Ma J, Alard P, Sokoloski KJ, Mathiowitz E, Furtado S, Egilmez NK, Kosiewicz MM. Male microbiota-associated metabolite restores macrophage efferocytosis in female lupus-prone mice via activation of PPAR $\gamma$ /LXR signaling pathways. *J Leukocyte Biol.* **2023**;113(1):41–57. doi: [10.1093/jleuko/qiac002](https://doi.org/10.1093/jleuko/qiac002)